International Journal of Pure and Applied Mathematics
Volume 104 No. 3 2015, 471-494
ISSN: 1311-8080 (printed version); ISSN: 1314-3395 (on-line version)
url: http://www.ijpam.eu
doi: http://dx.doi.org/10.12732/ijpam.v104i3.14

A MODIFIED P_1 – IMMERSED FINITE ELEMENT METHOD

Do Y. Kwak[1] §, Juho Lee[2]

[1,2]Department of Mathematical Sciences
KAIST, 291 Daehak-ro, Yuseong-gu
Daejeon, 305-701, KOREA

Abstract: In recent years, the immersed finite element methods (IFEM) introduced in [20], [21] to solve elliptic problems having an interface in the domain due to the discontinuity of coefficients are getting more attentions of researchers because of their simplicity and efficiency. Unlike the conventional finite element methods, the IFEM allows the interface to cut through the interior of the element, yet after the basis functions are altered so that they satisfy the flux jump conditions, it seems to show a reasonable order of convergence.

In this paper, we propose an improved version of the P_1 based IFEM by adding the line integral of flux terms on each element. This technique resembles the discontinuous Galerkin (DG) method, however, our method has much less degrees of freedom than the DG methods since we use the same number of unknowns as the conventional P_1 finite element method.

We prove H^1 and L^2 error estimates which are optimal both in order and regularity. Numerical experiments were carried out for several examples, which show the robustness of our scheme.

AMS Subject Classification: 65N30, 74S05, 76S05
Key Words: modified P_1-immersed finite element, flux jump, discontinuous Galerkin, NIPG, SIPG

1. Introduction

In recent years, there have been some developments of immersed finite element

Received: August 24, 2015

§Correspondence author

methods for elliptic problems having an interface. These methods use meshes which do not necessarily align with the discontinuities of the coefficients [20], [21], thus violate a basic principle of triangulations in the conventional finite element methods [4], [11]. However, when the basis functions are modified so that they satisfy the interface conditions, they seem to work well [10], [20], [21]. These methods were extended to the case of Crouzeix-Raviart P_1 nonconforming finite element method [12] by Kwak et al. [18], and to the problems with nonzero jumps in [7]. Some related works on interface problems can be found in [5], [16], [17], [19], [22], [23],[26].

On the other hand, the discontinuous Galerkin methods (DG) where one uses completely discontinuous basis functions were developed and have been studied extensively, see [1], [2], [13], [24] and references therein. The DG methods work quite well for problems with discontinuous coefficient in the sense that they capture the sharp changes of the solutions well, yet they require large number of unknowns and the meshes have to be aligned with the discontinuity.

The purpose of this paper is to combine the advantages of the two methods. We use a DG type idea of adding the consistency terms to the IFEM, thus proposing a modified version of IFEM based on the P_1 - Lagrange basis functions on triangular grids. In spirit, it resembles [15] in the sense that the standard linear basis functions are used for noninterface elements and line integrals are added, but in our method the line integrals along the edges, not along the interface, are added. Furthermore, our method incorporate the flux jump conditions to the basis functions hence requires no extra unknowns along the interface as in [15].

We prove error estimates in the mesh dependent H^1 - norm and L^2 - norm which are optimal both in the order and the regularity. We carry out various numerical tests to confirm our theory and compare the performance with the unmodified scheme.

2. Preliminaries

Let Ω be a connected, convex polygonal domain in $\mathbb{R}^2$ which is divided into two subdomains Ω^+ and Ω^- by a C^2 interface $\Gamma = \partial\Omega^+ \cap \partial\Omega^-$, see Figure 1. We assume that $\beta(x)$ is a positive function bounded below and above by two positive constants. Although our theory applies to the case of nonconstant $\beta(x)$, we assume $\beta(x)$ is piecewise constant for the simplicity of presentation: there are two positive constants β^+, β^- such that $\beta(x) = \beta^+$ on Ω^+ and $\beta(x) = \beta^-$

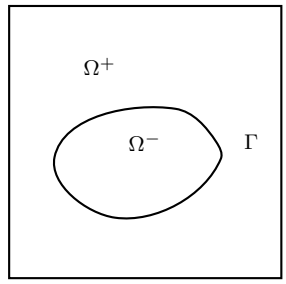

Figure 1: A domain Ω with interface

on Ω^-. Consider the following elliptic interface problem

$$-\nabla \cdot (\beta(x)\nabla u) = f \text{ in } \Omega^s \quad (s = +, -) \tag{2.1}$$

$$u = 0 \text{ on } \partial\Omega \tag{2.2}$$

with the jump conditions along the interface

$$[u]_\Gamma = 0, \quad \left[\beta(x)\frac{\partial u}{\partial n}\right]_\Gamma = 0, \tag{2.3}$$

where $f \in L^2(\Omega)$ and $u \in H_0^1(\Omega)$ and the bracket $[\cdot]_\Gamma$ means the jump across the interface:

$$[u]_\Gamma := u|_{\Omega^+} - u|_{\Omega^-}.$$

Let $p \geq 1$ and $m \geq 0$ be an integer. For any domain D, we let $W_p^m(D)$ be the usual Sobolev space with (semi)-norms and denoted by $|\cdot|_{m,p,D}$ and $\|\cdot\|_{m,p,D}$.

For $m \geq 1$, let

$$\widetilde{W}_p^m(D) := \{\, u \in W_p^{m-1}(D) : u|_{D\cap\Omega^s} \in W_p^m(D \cap \Omega^s), s = +, - \,\},$$

with norms;

$$|u|^p_{\widetilde{W}_p^m(D)} := |u|^p_{m,p,T\cap\Omega^+} + |u|^p_{m,p,D\cap\Omega^-},$$

$$\|u\|^p_{\widetilde{W}_p^m(D)} := \|u\|^p_{m-1,p,D} + |u|^p_{\widetilde{W}_p^m(D)}.$$

When $p = 2$, we write $\widetilde{H}^m(D)$ and denote the (semi)-norms by $|u|_{\widetilde{H}^m(D)}$ and $\|u\|_{\widetilde{H}^m(D)}$. $H_0^1(\Omega)$ is the subspace of $H^1(\Omega)$ with zero trace on the boundary.

Also, when some finite element triangulation $\{\mathcal{T}_h\}$ is involved, the norms are understood as piecewise norms $(\sum_{T\in\mathcal{T}_h} |u|^p_{\widetilde{W}^m_p(T)})^{1/p}$ and $(\sum_{T\in\mathcal{T}_h} \|u\|^p_{\widetilde{W}^m_p(T)})^{1/p}$, etc. If $p = 2$, we denote them by $|u|_{m,h}$ and $\|u\|_{m,h}$. We also need some subspaces of $\widetilde{H}^2(T)$ and $\widetilde{H}^2(\Omega)$ satisfying the jump conditions:

$$\begin{aligned}\widetilde{H}^2_\Gamma(T) &:= \{\, u \in H^1(T) :\, u|_{T\cap\Omega^s} \in H^2(T\cap\Omega^s),\\ &\qquad s = +,-,\quad \left[\beta\frac{\partial u}{\partial n}\right]_\Gamma = 0 \text{ on } \Gamma\cap T\,\}\\ \widetilde{H}^2_\Gamma(\Omega) &:= \{\, u \in H^1_0(\Omega) :\, u|_T \in \widetilde{H}^2_\Gamma(T),\ \forall T \in \mathcal{T}_h\}.\end{aligned}$$

Throughout the paper, the constants C, C_0, C_1, etc., are generic constants independent of the mesh size h and functions u, v but may depend on the problem data β, f and Ω, and are not necessarily the same on each occurrence.

The usual weak formulation for the problem (2.1) - (2.3) is: Find $u \in H^1_0(\Omega)$ such that

$$\int_\Omega \beta(x)\nabla u\cdot\nabla v dx = \int_\Omega fv dx, \quad \forall v \in H^1_0(\Omega). \tag{2.4}$$

We have the following existence and regularity theorem for this problem; see [5], [8], [25].

Theorem 2.1. *Assume that $f \in L^2(\Omega)$. Then the variational problem (2.4) has a unique solution $u \in \widetilde{H}^2(\Omega)$ which satisfies*

$$\|u\|_{\widetilde{H}^2(\Omega)} \le C\|f\|_{L^2(\Omega)}. \tag{2.5}$$

3. P_1-Immersed Finite Element Methods

We briefly review the immersed finite element space based on the P_1 - Lagrange basis functions ([20], [21]). Let $\{\mathcal{T}_h\}$ be the usual quasi-uniform triangulations of the domain Ω by the triangles of maximum diameter h which may not be aligned with the interface Γ. We call an element $T \in \mathcal{T}_h$ an *interface element* if the interface Γ passes through the interior of T, otherwise we call it a *noninterface* element. Let $\mathcal{T}^I_h$ be the collection of all interface elements. We assume that the interface meets the edges of an interface element at no more than two points.

We construct the local basis functions on each element T of the partition $\mathcal{T}_h$. For a noninterface element $T \in \mathcal{T}_h$, we simply use the standard linear shape functions on T whose degrees of freedom are functional values on the vertices

of T, and use $\overline{S}_h(T)$ to denote the linear spaces spanned by the three nodal basis functions on T:

$$\overline{S}_h(T) = \text{span}\{\, \phi_i \,:\, \phi_i \text{ is the standard linear shape function}\,\}$$

We let $\overline{S}_h(\Omega)$ denote the space of usual continuous, piecewise linear polynomials with vanishing boundary values.

Now we consider a typical interface element $T \in \mathcal{T}_h^I$ whose geometric configuration is given as in Fig. 2. Here the curve between the two points D and E is a part of the interface and $\overline{DE}$ is the line segment connecting the intersections of the interface and the edges.

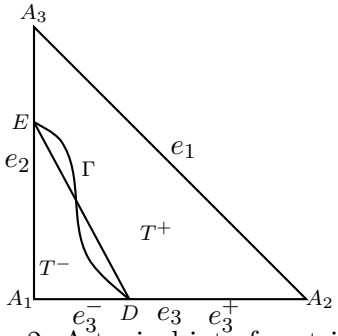

Figure 2: A typical interface triangle

We construct piecewise linear basis functions $\hat{\phi}_i, i = 1, 2, 3$ of the form

$$\hat{\phi}_i(X) = \begin{cases} a^+ + b^+x + c^+y, & X = (x, y) \in T^+, \\ a^- + b^-x + c^-y, & X = (x, y) \in T^-, \end{cases} \tag{3.1}$$

satisfying

$$\hat{\phi}_i(A_j) = \delta_{ij}, \quad j = 1, 2, 3, \tag{3.2}$$

$$[\hat{\phi}_i(D)] = [\hat{\phi}_i(E)] = 0, \tag{3.3}$$

$$\left[\beta \frac{\partial \hat{\phi}_i}{\partial \mathbf{n}}\right]_{\overline{DE}} = 0. \tag{3.4}$$

These are continuous, piecewise linear functions on T satisfying the flux jump condition along $\overline{DE}$, whose uniqueness and existence are known [10], [20].

Remark 3.1. Since $\hat{\phi}_i$ is continuous, piecewise linear, it is clear that the tangential derivative along $\overline{DE}$ is continuous, i.e.,

$$\frac{\partial \hat{\phi}_i^+}{\partial \mathbf{t}_{\overline{DE}}} = \frac{\partial \hat{\phi}_i^-}{\partial \mathbf{t}_{\overline{DE}}},$$

where $\mathbf{t}_{\overline{DE}}$ is the tangential vector to $\overline{DE}$.

We denote by $\widehat{S}_h(T)$ the space of functions generated by $\hat{\phi}_i$, $i = 1, 2, 3$ constructed above. Next we define the global *immersed finite element space* $\widehat{S}_h(\Omega)$ to be the set of all functions $\phi \in L^2(\Omega)$ such that

$$\left\{ \begin{array}{l} \phi \in \widehat{S}_h(T) \text{ if } T \in \mathcal{T}_h^I, \text{ and } \phi \in \overline{S}_h(T) \text{ if } T \notin \mathcal{T}_h^I, \\ \text{having continuity at all vertices of the triangulation} \\ \text{and vanishes on the boundary vertices.} \end{array} \right\}$$

We note that a function in $\widehat{S}_h(\Omega)$, in general, is not continuous across an edge common to two interface elements. Let $H_h(\Omega) := H_0^1(\Omega) + \widehat{S}_h(\Omega)$ and equip it with the piecewise norms $|u|_{1,h} := |u|_{\widetilde{H}^1(\Omega)}$, $\|u\|_{1,h} := \|u\|_{\widetilde{H}^1(\Omega)}$. Next, we define the interpolation operator. For any $u \in \widetilde{H}_\Gamma^2(T)$, we let $\hat{I}_h u \in \widehat{S}_h(T)$ be such that

$$\hat{I}_h u(A_i) = u(A_i), \quad i = 1, 2, 3,$$

where A_i, $i = 1, 2, 3$ are the vertices of T and we call $\hat{I}_h u$ the local *interpolant* of u in $\widehat{S}_h(T)$. We naturally extend it to $\widetilde{H}_\Gamma^2(\Omega)$ by $(\hat{I}_h u)|_T = \hat{I}_h(u|_T)$ for each T. Then we have the following approximation property [18], [21].

Proposition 3.2. *There exists a constant $C > 0$ such that*

$$\sum_{T \in \mathcal{T}_h} (\|u - \hat{I}_h u\|_{0,T} + h|u - \hat{I}_h u|_{1,T}) \leq Ch^2 \|u\|_{\widetilde{H}^2(\Omega)} \tag{3.5}$$

for all $u \in \widetilde{H}_\Gamma^2(\Omega)$.

With P_1- Lagrange basis function introduced in [20], [21], the IFEM reads: **(P_1-IFEM)** Find $u_h \in \widehat{S}_h(\Omega)$ such that

$$a_h(u_h, v_h) = (f, v_h), \quad \forall\, v_h \in \widehat{S}_h(\Omega), \tag{3.6}$$

where

$$a_h(u, v) = \sum_{T \in \mathcal{T}_h} \int_T \beta \nabla u \cdot \nabla v \, dx, \quad \forall\, u, v \in H_h(\Omega).$$

The error estimate for this scheme is shown in [10].

4. Modified P_1-IFEM

In this section, we modify the P_1-IFEM above by adding the line integrals for jumps of fluxes and functional values. The method resembles the discontinuous Galerkin methods (see [2], [14], [24] and references therein) which use completely discontinuous basis functions, but the degrees of freedom in our method are much smaller than the DG methods since our method has the same number of basis functions as the conventional P_1-FEM.

In order to describe the new method, we need some additional notations. Let the collection of all the edges of $T \in \mathcal{T}_h$ be denoted by $\mathcal{E}_h$ and we split $\mathcal{E}_h$ into two disjoint sets; $\mathcal{E}_h = \mathcal{E}_h^o \cup \mathcal{E}_h^b$, where $\mathcal{E}_h^o$ is the set of edges lying in the interior of Ω, and $\mathcal{E}_h^b$ is the set of edges on the boundary of Ω. In particular, we denote the set of edges cut by the interface Γ by $\mathcal{E}_h^I$. For every $e \in \mathcal{E}_h^o$, there are two element T_1 and T_2 sharing e as a common edge. Let $\mathbf{n}_{T_i}, i = 1, 2$ be the unit outward normal vector to the boundary of T_i, but for the edge e, we choose a direction of the normal vector, say $\mathbf{n}_e = \mathbf{n}_{T_1}$ and fix it once and for all. For functions v defined on $T_1 \cup T_2$, we let $[\cdot]_e$ and $\{\cdot\}_e$ denote the jump and average across e respectively, i.e.

$$[v]_e = v^1 - v^2, \{v\}_e = \frac{1}{2}(v^1 + v^2).$$

We also need the mesh dependent norm $|\!|\!| \cdot |\!|\!|$ on the space $H_h(\Omega)$,

$$\begin{aligned} |\!|\!| v |\!|\!|^2 \;:=\; & \sum_{T\in\mathcal{T}_h} \left(\left\| \sqrt{\beta} v \right\|_{0,T}^2 + \left\| \sqrt{\beta} \nabla v \right\|_{0,T}^2 \right) \\ & + \sum_{e\in\mathcal{E}_h^o} \left(h \left\| \{\sqrt{\beta}\nabla v \;\cdot \mathbf{n}_e\}_e \right\|_{0,e}^2 + h^{-1} \left\| [\sqrt{\beta} v]_e \right\|_{0,e}^2 \right). \end{aligned}$$

Multiplying both sides of the equation (2.1) by $v \in H^1(T)$, applying Green's formula and adding, we get

$$\sum_{T\in\mathcal{T}_h} \left(\int_T \beta \nabla u \cdot \nabla v dx - \int_{\partial T} \beta \nabla u \cdot \mathbf{n}_T \, v ds \right) = \int_\Omega f v dx.$$

By using the preassigned normal vectors $\mathbf{n}_e$ and adding the unharmful term $\epsilon \int_e \{\beta \nabla v \cdot \mathbf{n}_e\}_e [u]_e$ for any ϵ, we see the above equation becomes

$$\sum_{T\in\mathcal{T}_h} \int_{\mathcal{T}} \beta \nabla u \cdot \nabla v dx - \sum_{e\in\mathcal{E}_h^o} \int_e \{\beta \nabla u \cdot \mathbf{n}_e\}_e [v]_e ds$$

$$+\epsilon \sum_{e\in\mathcal{E}_h^o}\int_e \{\beta\nabla v\cdot\mathbf{n}_e\}_e[u]_e ds = \int_\Omega fv dx \quad (4.1)$$

which is valid for $v \in L^2(\Omega)$ such that $v \in H^1(T)$ for all $T \in \mathcal{T}_h$. We define the following bilinear forms

$$\begin{aligned} b_\epsilon(u,v) &:= -\sum_{e\in\mathcal{E}_h^o}\int_e \{\beta\nabla u\cdot\mathbf{n}_e\}_e[v]_e ds + \epsilon\sum_{e\in\mathcal{E}_h^o}\int_e \{\beta\nabla v\cdot\mathbf{n}_e\}_e[u]_e ds,\\ j_\sigma(u,v) &:= \sum_{e\in\mathcal{E}_h^o}\int_e \frac{\sigma}{h}[u]_e[v]_e ds, \text{ for some } \sigma>0\\ a_\epsilon(u,v) &:= a_h(u,v)+b_\epsilon(u,v)+j_\sigma(u,v). \end{aligned}$$

Now, for each $\epsilon = 0$, $\epsilon = -1$ and $\epsilon = 1$, we define the modified P_1-IFEM for the problem (2.1)-(2.3):

(Modified P_1-IFEM) Find $u_h^m \in \widehat{S}_h(\Omega)$ such that

$$a_\epsilon(u_h^m, v_h) = (f, v_h), \quad \forall v_h \in \widehat{S}_h(\Omega). \quad (4.2)$$

This is similar to a class of DG methods, corresponding to IP, SIPG, NIPG and OBB ([1], [14], [13], [3]), if $\epsilon = 0$, $\epsilon = -1$, $\epsilon = 1$, and $\epsilon = 0, \sigma = 0$, respectively.

Remark 4.1. For the line integrals in $b_\epsilon(u,v)$, it suffices to consider the integrals on the edges of the interface elements only since both $[u_h], [v_h]$ vanish for $e \in \mathcal{E}_h^o \setminus \mathcal{E}_h^I$.

5. Error Analysis

In this section, we prove an optimal order of error estimates in H^1 and L^2-norms of our schemes. For simplicity, we present the case with $\epsilon = -1$ only. All other cases are similar. Also, we assume the smooth interface is replaced by piecewise line segment on each element.

We need the well-known inverse inequality and trace theorem ([1], [11]):

Lemma 5.1. *There exist positive constants C_0, C_1 independent of the function v_h such that for all $v_h \in P_k(T) \cup \hat{S}_h(T)$,*

$$\|v_h\|_{1,T}^2 \le C_0 h^{-2}\|v_h\|_{0,T}^2, \quad \|v_h\|_{0,\partial T}^2 \le C_1 h^{-1}\|v_h\|_{0,T}^2. \quad (5.1)$$

There exists a positive constant C_2 independent of the function v such that for all $v \in H^1(T)$

$$\|v\|_{0,e}^2 \le C_2(h^{-1}\|v\|_{0,T}^2 + h|v|_{1,T}^2). \quad (5.2)$$

Now we show the following interpolation error estimate for the mesh dependent norm $|\!|\!| \cdot |\!|\!|$.

Proposition 5.2. *There exist positive constants C, C_I independent of the function u such that for all $u \in H^1(\Omega) \cap \widetilde{H}^2_\Gamma(\Omega)$,*

$$\sum_{e\in\mathcal{E}_h^o} h \left\| \{\nabla(u - \hat{I}_h u)\cdot \mathbf{n}_e\}_e \right\|^2_{0,e} + \sum_{e\in\mathcal{E}_h^o} h^{-1} \left\| [u - \hat{I}_h u]_e \right\|^2_{0,e} \le Ch^2 \|u\|^2_{\widetilde{H}^2(\Omega)}. \quad (5.3)$$

Consequently, we have

$$|\!|\!| u - \hat{I}_h u |\!|\!| \le C_I h \|u\|_{\widetilde{H}^2(\Omega)}. \quad (5.4)$$

Proof. We first consider $\nabla(u - \hat{I}_h u)$. Since $\nabla(u - \hat{I}_h u)$ is not in $H^1(T)$, we cannot apply (5.2) directly. Instead, we decompose it as

$$\nabla(u - \hat{I}_h u) = (\nabla(u - \hat{I}_h u)\cdot \mathbf{n}_\Gamma)\mathbf{n}_\Gamma + (\nabla(u - \hat{I}_h u)\cdot \mathbf{t}_\Gamma)\mathbf{t}_\Gamma := \mathbf{w} + \mathbf{z},$$

where $\mathbf{n}_\Gamma$ and $\mathbf{t}_\Gamma$ are the unit normal and tangent vector to the interface Γ, respectively. We have

$$\begin{aligned} \left\| \nabla(u - \hat{I}_h u)\cdot \mathbf{n}_e \right\|^2_{0,e} &\le \|\mathbf{w}\cdot\mathbf{n}_e\|^2_{0,e} + \|\mathbf{z}\cdot\mathbf{n}_e\|^2_{0,e} \\ &\le \frac{1}{\beta^2_{min}} \|\beta\mathbf{w}\cdot\mathbf{n}_e\|^2_{0,e} + \|\mathbf{z}\cdot\mathbf{n}_e\|^2_{0,e}. \end{aligned}$$

We can easily check that $\beta\mathbf{w}$ is in $H^1(T)$. For the smoothness of $\mathbf{z}$ we proceed as follows: Since $u \in H^1(T)$, we have $(\nabla u\cdot\mathbf{t}_\Gamma)|_{T^+\cap\Gamma} = (\nabla u\cdot\mathbf{t}_\Gamma)|_{T^-\cap\Gamma}$. Hence $(\nabla u\cdot\mathbf{t}_\Gamma)|_T$ has well defined trace on Γ, which implies $\nabla u\cdot\mathbf{t}_\Gamma$ is in $\tilde{H}^1(T)$ also. Therefore, we can apply (5.2) to $\beta\mathbf{w}\cdot\mathbf{n}_e$ and $\mathbf{z}\cdot\mathbf{n}_e$. Hence

$$\begin{aligned} & h \left\| \nabla(u - \hat{I}_h u)\cdot \mathbf{n}_e \right\|^2_{0,e} \\ \le\ & \frac{C_2}{\beta^2_{min}} \left(\|\beta\mathbf{w}\cdot\mathbf{n}_e\|^2_{0,T} + h^2 |\beta\mathbf{w}\cdot\mathbf{n}_e|^2_{1,T} \right) + C_2 \left(\|\mathbf{z}\cdot\mathbf{n}_e\|^2_{0,T} + h^2 |\mathbf{z}\cdot\mathbf{n}_e|^2_{1,T} \right) \\ \le\ & C_2 \left(\frac{\beta^2_{max}}{\beta^2_{min}} \left(\|\mathbf{w}\|^2_{0,T} + h^2 |\mathbf{w}|^2_{\tilde{H}^1(T)} \right) + \|\mathbf{z}\|^2_{0,T} + h^2 |\mathbf{z}|^2_{\tilde{H}^1(T)} \right) \\ \le\ & C_2\ \alpha^2 \left(\left\| \nabla(u - \hat{I}_h u) \right\|^2_{0,T} + h^2 \left| \nabla(u - \hat{I}_h u) \right|^2_{\tilde{H}^1(T)} \right) \\ \le\ & Ch^2 \|u\|^2_{\tilde{H}^2(T)}, \end{aligned}$$

where $\beta_{min} = \min(\beta^+, \beta^-)$, $\beta_{max} = \max(\beta^+, \beta^-)$ and we have set $\alpha = \frac{\beta_{max}}{\beta_{min}}$. Here Proposition 3.2 was used to derive the last estimate.

The estimate of the second term follows easily from (5.2) and Proposition 3.2:

$$\begin{aligned} h^{-1} \left\| u - \hat{I}_h u \right\|^2_{0,\partial T} &\leq C_2 \left(h^{-2} \left\| u - \hat{I}_h u \right\|^2_{0,T} + \left| u - \hat{I}_h u \right|^2_{\tilde{H}^1(T)} \right) \\ &\leq C h^2 \|u\|^2_{\tilde{H}^2(T)}. \end{aligned}$$

Thus, the estimate (5.4) follows. □

The following discrete Poincaré inequality holds for $\hat{S}_h(\Omega)$, (see [10]).

Lemma 5.3. *There exists a constant $C_p > 0$ such that*

$$C_p \|v_h\|^2_{0,\Omega} \leq |v_h|^2_{1,h}, \qquad \forall v_h \in \hat{S}_h(\Omega). \tag{5.5}$$

Now we show some basic properties of $a_\epsilon(\cdot,\cdot)$. Clearly, $a_\epsilon(\cdot,\cdot)$ is bounded on $H_h(\Omega)$ with respect to $|\!|\!| \cdot |\!|\!|$:

$$|a_\epsilon(u,v)| \leq C_b |\!|\!| u |\!|\!| |\!|\!| v |\!|\!|, \qquad \forall u, v \in H_h(\Omega).$$

Next, we prove the coercivity of the form $a_\epsilon(\cdot,\cdot)$ on the space $\hat{S}_h(\Omega)$. We need a lemma.

Lemma 5.4. *For all $v \in \hat{S}_h(\Omega)$, there exists a positive constant C independent of h such that*

$$\sum_{e \in \mathcal{E}_h^o} h \left\| \left\{ \sqrt{\beta} \nabla v \cdot \mathbf{n} \right\} \right\|^2_{0,e} \leq C_1 \alpha \sum_{T \in \mathcal{T}_h} \left\| \sqrt{\beta} \nabla v \right\|^2_{0,T} \tag{5.6}$$

where $\alpha = \frac{\beta_{max}}{\beta_{min}}$ is the same as before.

Proof. We decompose ∇v_h as

$$\nabla v_h = (\nabla v_h \cdot \mathbf{n}_\Gamma)\mathbf{n}_\Gamma + (\nabla v_h \cdot \mathbf{t}_\Gamma)\mathbf{t}_\Gamma := \mathbf{w} + \mathbf{z}. \tag{5.7}$$

The rest of the proof is almost the same as that of (5.3). □

Proposition 5.5. *There exists a positive constant C_c independent of v_h such that for all $v_h \in \hat{S}_h(\Omega)$ the following holds:*

$$a_\epsilon(v_h, v_h) \geq C_c |\!|\!| v_h |\!|\!|^2.$$

Proof. First of all, we consider $b_\epsilon(v_h, v_h)$, the second part of $a_\epsilon(v_h, v_h)$. By Lemma 5.4, Cauchy-Schwarz and arithmetic-geometric inequality, we have

$$\begin{aligned}
&\sum_{e\in\mathcal{E}_h^o}\int_e \{\beta\nabla v_h\cdot\mathbf{n}\}\,[v_h]ds\\
\leq\ &\left(\sum_{e\in\mathcal{E}_h^o} h\,\|\{\beta\nabla v_h\cdot\mathbf{n}\}\|_{0,e}^2\right)^{1/2}\left(\sum_{e\in\mathcal{E}_h^o} h^{-1}\,\|[v_h]\|_{0,e}^2\right)^{1/2}\\
\leq\ &\left(C_1\alpha\sum_{T\in\mathcal{T}_h}\left\|\sqrt{\beta}\nabla v_h\right\|_{0,T}^2\right)^{1/2}\left(\sum_{e\in\mathcal{E}_h^o} h^{-1}\left\|[\sqrt{\beta}v_h]\right\|_{0,e}^2\right)^{1/2}\\
\leq\ &\frac{\gamma}{2}\left(\sum_{T\in\mathcal{T}_h}\left\|\sqrt{\beta}\nabla v_h\right\|_{0,T}^2\right)+\frac{C_1\alpha}{2\gamma}\left(\sum_{e\in\mathcal{E}_h^o} h^{-1}\left\|[\sqrt{\beta}v_h]\right\|_{0,e}^2\right)
\end{aligned}$$

for every $\gamma>0$. Hence by Lemma 5.3, we have

$$\begin{aligned}
a_\epsilon(v_h,v_h) &= a_h(v_h,v_h)+b_\epsilon(v_h,v_h)+j_\sigma(v_h,v_h)\\
&= \sum_{T\in\mathcal{T}_h}\int_T \beta\nabla v_h\cdot\nabla v_h\,dx-2\sum_{e\in\mathcal{E}_h^o}\int_e\{\beta\nabla v_h\cdot\mathbf{n}\}\,[v_h]ds+\sum_{e\in\mathcal{E}_h^o}\int_e\frac{\sigma}{h}[v_h]^2ds\\
&\geq \frac{C_p}{2}\left\|\sqrt{\beta}v_h\right\|_{0,\Omega}^2+(\frac{1}{2}-\gamma)\left|\sqrt{\beta}v_h\right|_{1,h}^2+\left(\sigma_0-\frac{C_1\alpha}{\gamma}\right)\sum_{e\in\mathcal{E}_h^o}\frac{1}{h}\left\|[\sqrt{\beta}v_h]\right\|_{0,e}^2\\
&\geq \frac{C_p}{2}\left\|\sqrt{\beta}v_h\right\|_{0,\Omega}^2+(\frac{1}{4}-\gamma)\left|\sqrt{\beta}v_h\right|_{1,h}^2+\frac{1}{4C_1\alpha}\sum_{e\in\mathcal{E}_h^o}h\left\|\left\{\sqrt{\beta}\nabla v_h\cdot\mathbf{n}\right\}\right\|_{0,e}^2\\
&\quad+\left(\sigma_0-\frac{C_1\alpha}{\gamma}\right)\sum_{e\in\mathcal{E}_h^o}\frac{1}{h}\left\|[\sqrt{\beta}v_h]\right\|_{0,e}^2,
\end{aligned}$$

where we have set $\sigma_0=\sigma/\beta$. If we choose $\gamma=\frac{1}{8}$ and σ_0 large enough so that $(\sigma_0-8C_1\alpha)\geq\frac{1}{8}$. Then with $C_c:=\min\left(\frac{C_p}{2},\,\frac{1}{8},\,\frac{1}{4C_1\alpha}\right)$, we have

$$a_\epsilon(v,v)\geq C_c|\!|\!|v|\!|\!|^2.$$

□

Remark 5.6. We can take any positive σ when $\epsilon=1$, because $b_\epsilon(v,v)$ becomes zero. If $\epsilon=0$ or -1, it seems that $\sigma>0$ must be large enough to show the coercivity. However, small positive σ or even $\sigma=0$ works for all the cases

we have tested. This is in contrast to the usual DG schemes, where sufficiently large σ is necessary. The reason seems to be that, unlike the usual DG, the term $b_\epsilon(v,v)$ is small enough to be dominated by $a_h(v,v)$, since the jump $[v]$ vanishes at the vertices of each $T \in \mathcal{T}_h$. In fact, using the technique in [9] and in the proof of Proposition 5.2 we can show $|b_\epsilon(v,v)| \le C(h|\log h|)^{1/2}\|v\|_{1,h}$, but the details are complicated. This will be shown in the subsequent paper.

5.1. H^1-Error Analysis

First we check that the modified P_1-IFEM is consistent.

Lemma 5.7. *Let u be the solution of (2.1)-(2.3) and let u_h^m be the solution of (4.2). For any $v_h \in \widehat{S}_h(\Omega)$, we have*

$$a_\epsilon(u, v_h) = (f, v_h). \tag{5.8}$$

In other words,

$$a_\epsilon(u - u_h^m, v_h) = 0.$$

Proof. By (4.1), the definition of the a_ϵ form and the homogeneous jump condition of u, we have

$$a_\epsilon(u, v_h) - a_\epsilon(u_h^m, v_h) = a_\epsilon(u, v_h) - (f, v_h) = \sum_{e \in \mathcal{E}_h^o} \int_e \frac{\sigma}{h}[u]_e[v_h]_e ds = 0.$$

□

Now we can prove the H^1-error estimate which is optimal both in order and the regularity.

Theorem 5.1. *Let u be the solution of (2.1)-(2.3) and let u_h^m be the solution of (4.2). Then there exists a positive constant C independent of u and h such that*

$$|\!|\!| u - u_h^m |\!|\!| \;\le\; Ch\|u\|_{\widetilde{H}^2(\Omega)}.$$

Proof. By Proposition 5.5, (5.8) and boundedness of $a_\epsilon(\cdot,\cdot)$ with respect to $|\!|\!|\cdot|\!|\!|$, we have

$$\begin{aligned} |\!|\!| u_h^m - \hat{I}_h u |\!|\!|^2 &\le C_c^{-1} a_\epsilon(u_h^m - \hat{I}_h u, u_h^m - \hat{I}_h u) \\ &= C_c^{-1} a_\epsilon(u - \hat{I}_h u, u_h^m - \hat{I}_h u) \end{aligned}$$

$$\leq C_c^{-1} C_b |\!|\!| u - \hat{I}_h u |\!|\!| |\!|\!| u_h^m - \hat{I}_h u |\!|\!|.$$

By the triangle inequality and Proposition 5.2, we get

$$\begin{aligned} |\!|\!| u - u_h^m |\!|\!| &\leq |\!|\!| u - \hat{I}_h u |\!|\!| + |\!|\!| u_h^m - \hat{I}_h u |\!|\!| \\ &\leq (C_c^{-1} C_b + 1) C_I h \|u\|_{\widetilde{H}^2(\Omega)}. \end{aligned}$$

□

5.2. L^2-Error Analysis

Theorem 5.2. *For the solution u_h^m of (4.2), there exists a positive constant C independent of u and h such that*

$$\|u - u_h^m\|_{L^2(\Omega)} \leq C h^2 \|u\|_{\widetilde{H}^2(\Omega)}.$$

Proof. Consider the dual equation:

$$\begin{aligned} -\nabla(\beta \nabla \Psi) &= w \quad \text{in } \Omega^s \ (s = +, -) \\ [\Psi]_\Gamma &= 0, \\ \left[\beta(x) \frac{\partial \Psi}{\partial n} \right]_\Gamma &= 0, \\ \Psi &= 0 \quad \text{on } \partial\Omega. \end{aligned}$$

Then by Theorem 2.1 the solution satisfies

$$\|\Psi\|_{\tilde{H}^2(\Omega)} \leq C \|w\|_{L^2(\Omega)}. \tag{5.9}$$

Let Ψ_h be the modified IFEM solution of this problem. Then with $e_h := u - u_h^m$, we have by Lemma 5.7

$$(e_h, w) = a_\epsilon(e_h, \Psi) = a_\epsilon(e_h, \Psi - \Psi_h).$$

Then by boundedness of a_ϵ, Theorem 5.1 and (5.9)

$$|(e_h, w)| \leq C |\!|\!| e_h |\!|\!| |\!|\!| \Psi - \Psi_h |\!|\!| \leq Ch \|\Psi\|_{\tilde{H}^2(\Omega)} |\!|\!| e_h |\!|\!| \leq Ch \|w\|_{L^2(\Omega)} |\!|\!| e_h |\!|\!|.$$

Taking $w = e_h$, we obtain

$$\|u - u_h^m\|_{L^2(\Omega)} \leq Ch |\!|\!| u - u_h^m |\!|\!| \leq Ch^2 \|u\|_{\widetilde{H}^2(\Omega)}.$$

□

6. Numerical Experiments

For numerical tests, we solve the problem (2.1)-(2.3) on the rectangular domain $\Omega = [-1,1] \times [-1,1]$ partitioned into unform right triangles with $h_x = h_y = 1/2^{n-1}$ for $n = 4, \cdots, 10$. Three types of interface problems are considered with various values of parameter β. We measured $\|u - u_h\|_0$ and $\|u - u_h\|_{1,h}$ which are very close to the theoretical orders of convergence, 2 and 1 respectively. Although not reported, we also measured $\sum_e \|u-u_h\|_{0,e}$ and $\sum_e \|\partial(u-u_h)/\partial n\|_{0,e}$, the orders of which agree with the theoretical value 1.5 and 0.5 respectively. Moreover, we observe the second order convergence in L^∞ norm also.

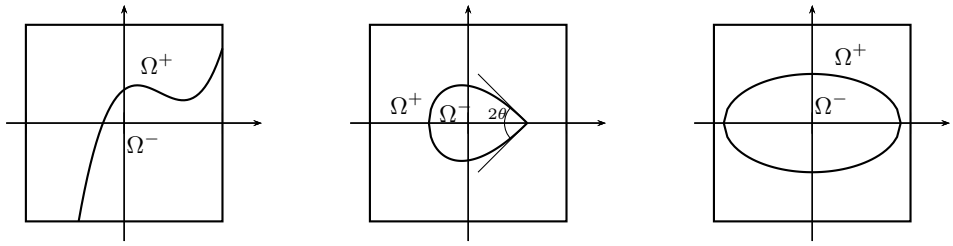

Figure 3: Interfaces of Examples 1,2 and 3

Example 6.1 (Cubic curve)**.** *The 0-set of function* $L(x,y) = y - 3x(x - 0.3)(x - 0.8) - 0.34$ *is used in this example as the interface. The exact solution is* $u = L(x,y)/\beta$*, where* $\beta = \beta^\pm$ *on* $\Omega^\pm$*. We test the cases when* $\beta^+/\beta^- = 10$ *and* 1000*.*

The comparison with error surfaces in Figure 5. shows that modified method gives much more accurate results than the original P_1-IFEM when $\beta^+/\beta^- = 10$ and $1/h_x = 128$. The smaller the mesh, the more accurate results the modified method shows.

Table 1 shows the comparison of errors between the two methods when $\beta^+/\beta^- = 10$. We can see the original P_1-IFEM has suboptimal convergence as the grids are refined ($1/h_x = 256$ and 512). However, the modified method shows a robust order of convergence for all grids.

On the other hands, Table 2 shows both methods has an optimal convergence in L^2 and H^1 norms when $\beta^+/\beta^- = 1000$.

Remark 6.1. Comparing Tables 1 and 2, we see the original P_1-IFEM behaves better when $\beta^+/\beta^- = 1000$ than $\beta^+/\beta^- = 10$. This is a common phenomenon for all the examples we tested. This seems to contradict the usual

	$1/h_x$	$\|u-u_h\|_0$	order	$\|u-u_h\|_{1,h}$	order	$\|u-u_h\|_\infty$	order
	8	1.344e-2		3.315e-1		2.761e-2	
	16	3.453e-3	1.961	1.709e-1	0.955	8.715e-3	1.663
P_1-IFEM	32	8.9002-4	1.956	8.727e-3	0.970	3.069e-3	1.506
	64	2.161e-4	2.043	4.507e-2	0.953	1.295e-3	1.245
	128	5.541e-5	1.963	2.347e-2	0.941	5.786e-4	1.162
	256	1.851e-5	1.582	1.288e-2	0.865	3.598e-4	0.686
	512	8.193e-6	1.176	7.297e-3	0.820	1.776e-4	1.018
	$1/h_x$	$\|u-u_h^m\|_0$	order	$\|u-u_h^m\|_{1,h}$	order	$\|u-u_h^m\|_\infty$	order
	8	1.233e-2		3.306e-1		2.345e-2	
	16	3.260e-3	1.919	1.694e-1	0.965	6.765e-3	1.793
Modified	32	8.269e-4	1.979	8.554e-2	0.986	1.775e-3	1.931
P_1-IFEM	64	2.094e-4	1.982	4.300e-2	0.992	4.621e-4	1.941
	128	5.286e-5	1.986	2.156e-2	0.996	1.185e-4	1.964
	256	1.328e-5	1.993	1.078e-2	0.999	2.991e-5	1.986
	512	3.308e-6	2.005	5.399e-3	0.998	7.557e-6	1.985

Table 1: Example 6.1 (Cubic curve): $\beta^- = 1,\ \beta^+ = 10$

	$1/h_x$	$\|u-u_h\|_0$	order	$\|u-u_h\|_{1,h}$	order	$\|u-u_h\|_\infty$	order
	8	1.923e-2		3.530e-1		5.617e-2	
	16	4.002e-3	2.264	1.716e-1	1.040	1.470e-2	1.934
P_1-IFEM	32	9.196e-4	2.122	8.453e-2	1.022	3.854e-3	1.932
	64	2.291e-4	2.005	4.221e-2	1.002	1.288e-3	1.582
	128	5.408e-5	2.083	2.105e-2	1.004	2.836e-4	2.183
	256	1.337e-5	2.016	1.056e-2	0.995	1.159e-4	1.291
	512	3.336e-6	2.002	5.304e-3	0.994	5.258e-5	1.141
	$1/h_x$	$\|u-u_h^m\|_0$	order	$\|u-u_h^m\|_{1,h}$	order	$\|u-u_h^m\|_\infty$	order
	8	1.266e-2		3.216e-1		2.470e-2	
	16	3.205e-3	1.982	1.643e-1	0.969	6.836e-3	1.854
Modified	32	8.163e-4	1.973	8.293e-2	0.986	1.784e-3	1.938
P_1-IFEM	64	2.068e-4	1.981	4.172e-2	0.991	4.642e-4	1.943
	128	5.199e-5	1.992	2.093e-2	0.996	1.185e-4	1.970
	256	1.302e-5	1.998	1.048e-2	0.998	3.009e-5	1.977
	512	3.259e-6	1.998	5.243e-3	0.999	7.564e-6	1.992

Table 2: Example 6.1 (Cubic curve) : $\beta^- = 1,\ \beta^+ = 1000$

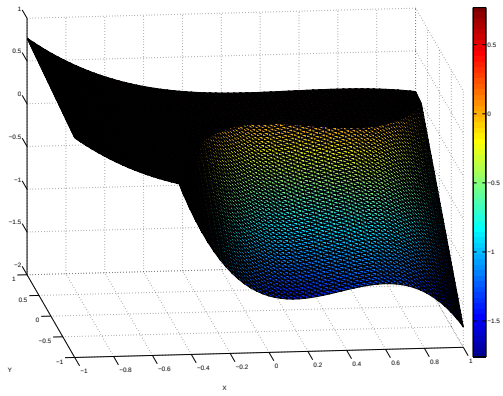

Figure 4: Solution u_h for Example 6.1 ($\beta^- = 1$, $\beta^+ = 10$, $1/h_x = 32$)

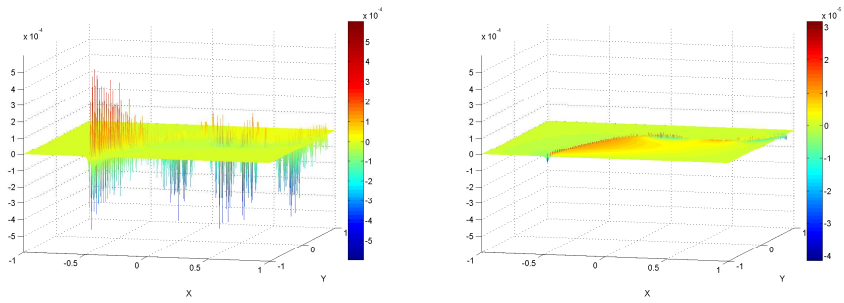

(a) P_1-IFEM (b) Modified P_1-IFEM

Figure 5: Error Surface for Example 6.1 (Cubic Curve)
($\beta^- = 1$, $\beta^+ = 10$, $1/h_x = 128$)

behavior of standard FEM. We guess the reason is that the large ratio between the coefficients masks the discontinuity of basis functions. Figure 6 shows the behavior of P_1-IFEM basis between $\beta^+/\beta^- = 10$ and $\beta^+/\beta^- = 1000$. When $\beta^+/\beta^- = 10$, the gap between adjacent elements is conspicuous. However, when $\beta^+/\beta^- = 1000$, the gap is almost invisible.

Example 6.2 (Sharp corner)**.** *In this example, we consider an interface with a sharp corner having interior angle* 2θ*. Let* Γ *be the zero set of* $L(x, y) = -y^2 + ((x - 0.6)\tan\theta)^2(x + 0.4)$ *for* $x \le 0.6$*. We test the case with* $\theta = 45°$ *and* $\beta^+/\beta^- = 10$ *and* $1/10$*. The exact solution is* $u = L(x, y)/\beta$*.*

This example is not covered by analysis of this work because the problem

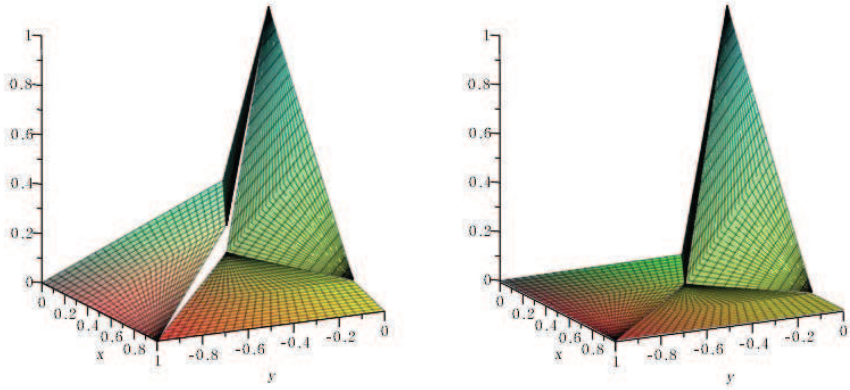

(a) $\beta^+/\beta^- = 10$ (b) $\beta^+/\beta^- = 1000$

Figure 6: Comparison of P_1-IFEM basis with different β^+/β^-

	$1/h_x$	$\|u-u_h\|_0$	order	$\|u-u_h\|_{1,h}$	order	$\|u-u_h\|_\infty$	order
P_1-IFEM	8	3.359e-3		7.958e-2		1.036e-2	
	16	9.014e-4	1.898	4.185e-3	0.927	4.118e-3	1.332
	32	2.219e-4	2.022	2.161e-3	0.954	1.958e-3	1.073
	64	5.686e-5	1.965	1.197e-3	0.852	9.568e-4	1.033
	128	1.463e-5	1.958	6.573e-3	0.865	5.063e-4	0.918
	256	6.070e-6	1.269	3.967e-3	0.728	2.462e-4	1.040
	512	2.942e-6	1.045	2.439e-3	0.702	1.241e-4	0.988
	$1/h_x$	$\|u-u_h^m\|_0$	order	$\|u-u_h^m\|_{1,h}$	order	$\|u-u_h^m\|_\infty$	order
Modified P_1-IFEM	8	3.056e-3		7.817e-2		9.005e-3	
	16	7.441e-4	2.038	3.956e-2	0.983	2.316e-3	1.959
	32	1.930e-4	1.947	1.990e-2	0.991	6.221e-4	1.896
	64	4.716e-5	2.033	1.000e-2	0.993	1.608e-4	1.952
	128	1.216e-5	1.956	5.015e-3	0.996	4.090e-5	1.975
	256	3.010e-6	2.014	2.510e-3	0.999	1.031e-5	1.989
	512	7.621e-7	1.982	1.256e-3	0.999	2.633e-6	1.968

Table 3: Example 6.2 (Sharp corner) : $\theta = 45°,\ \beta^- = 1,\ \beta^+ = 10$

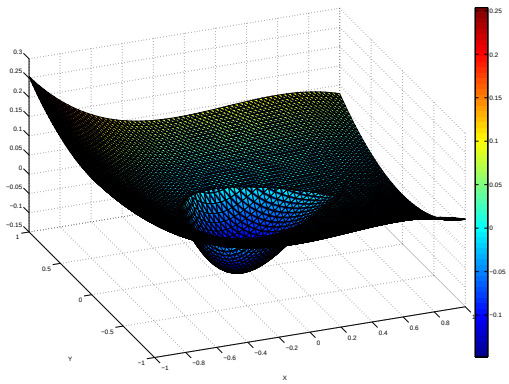

Figure 7: Solution u_h for Example 6.2 (Sharp Corner)
($\beta^- = 1$, $\beta^+ = 10$, $\theta = 45°$, $1/h_x = 32$)

has low regularity at the interface corner. However, we see that the modified method works better; See the Table 3.

Remark 6.2. We have also computed other cases such as $\beta^+/\beta^- = 1000, 0.001$ with various angles. The results of our scheme are always optimal while the unmodified P_1 immersed method deteriorates for some cases.

Example 6.3 (Variable coefficient)**.** *Finally, we consider the case with variable coefficient. The 0-set of function* $L(x,y) = x^2/(0.9)^2 + y^2/(0.5)^2 - 1.0$ *is used in this example as the interface. The exact solution is* $u = L(x,y)/\beta(x,y)$ *where*

$$\beta(x,y) = \begin{cases} (x^2+y^2-1)^2 & \text{on } \Omega^-, \\ 1 & \text{on } \Omega^+. \end{cases}$$

In this case, both methods show an optimal order of convergence in H^1*-norm. But the modified method performs much better in* L^∞*-norm; See Table 5.*

7. Conclusion

We introduced a modified IFEM for solving elliptic interface problems. By adding the line integral terms similar to the DG methods, we overcome the suboptimal behavior of the original IFEM proposed in [20], [21]. (The computational result there seemed to show optimal order. However, more numerical

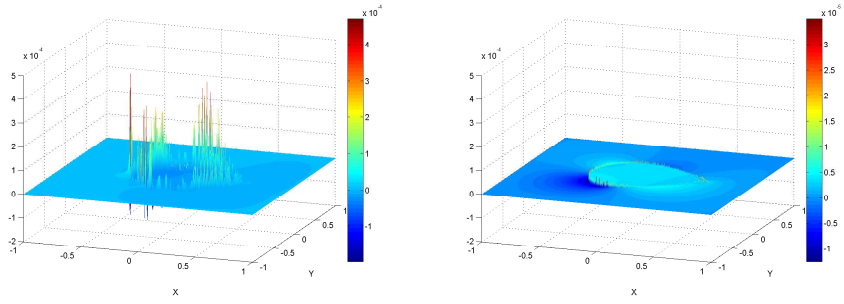

(a) P_1-IFEM (b) Modified P_1-IFEM

Figure 8: Error Surfaces for Example 6.2 (sharp corner)
($\beta^- = 1$, $\beta^+ = 10$, $\theta = 45°$, $1/h_x = 128$)

	$1/h_x$	$\|u - u_h\|_0$	order	$\|u - u_h\|_{1,h}$	order	$\|u - u_h\|_\infty$	order
P_1-IFEM	8	1.238e-2		3.013e-1		1.613e-2	
	16	3.159e-3	1.971	1.513e-1	0.994	4.327e-3	1.899
	32	7.949e-4	1.991	7.572e-2	0.998	1.174e-3	1.882
	64	2.030e-4	1.969	3.821e-2	0.987	7.475e-4	0.651
	128	5.366e-5	1.920	1.933e-2	0.983	4.704e-4	0.668
	256	1.528e-5	1.812	9.919e-3	0.963	2.452e-4	0.940
	512	4.898e-6	1.642	5.155e-3	0.944	1.199e-4	1.033
	$1/h_x$	$\|u - u_h^m\|_0$	order	$\|u - u_h^m\|_{1,h}$	order	$\|u - u_h^m\|_\infty$	order
Modified P_1-IFEM	8	1.238e-2		3.010e-1		1.610e-2	
	16	3.094e-3	2.000	1.507e-1	0.998	4.107e-3	1.971
	32	7.787e-4	1.990	7.543e-2	0.999	1.037e-3	1.986
	64	1.947e-4	2.000	3.773e-2	0.999	2.605e-4	1.993
	128	4.876e-5	1.998	1.887e-2	1.000	6.528e-5	1.997
	256	1.219e-5	2.000	9.435e-3	1.000	1.634e-5	1.998
	512	3.051e-6	1.998	4.718e-3	1.000	4.087e-6	1.999

Table 4: Example 6.2 (Sharp corner) : $\theta = 45°$, $\beta^- = 10$, $\beta^+ = 1$

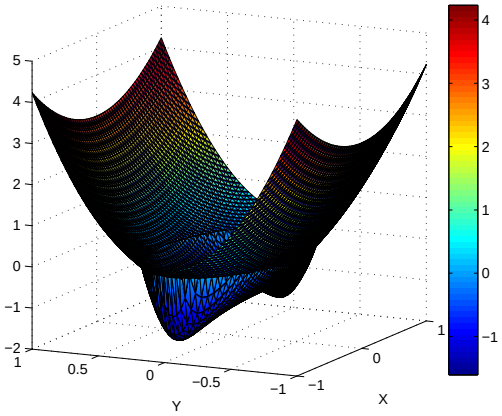

Figure 9: Solution u_h for Example 6.3 (Variable coefficient)

experiments show the original P_1-IFEM is not optimal for some problems. The proof in [10] seems incorrect. However, our modified scheme is always robust for all problems tested including unreported ones). The optimal convergence rates in H^1 and L^2 norms are shown by a similar technique as in DG methods; the modified IFEM is consistent, the coercivity and boundedness of the bilinear form hold. Several numerical tests show the errors are $O(h)$, $O(h^2)$ order in respective norms. Although no proof is given, we also obtain $O(h^2)$ order in L^∞ norm.

Some of the limitation of our scheme might be these: for problems with sharp interface, one has to arrange the grids so that the cusp point is located at a vertex of an element, for problems with highly oscillating interface, further refinement are necessary to apply the IFEM.

We now comment on the computational aspects: The matrix structure are exactly the same as usual P_1-FEM, i.e., 5-point stencil; the number of unknowns are also the same. When $\epsilon = -1$, the scheme becomes symmetric. The assembly of stiffness matrix requires slightly more time than the unmodified P_1-IFEM, but the time for iterative solver such as conjugate gradient is almost the same.

An obvious advantage of (both) IFEM is that we can use fast solver such as multigrid methods since we can use uniform meshes.

Future works related to this topic are:

1. Local refinement near singularity.

2. Problems with nonhomogenous jumps, tensor coefficients, etc.

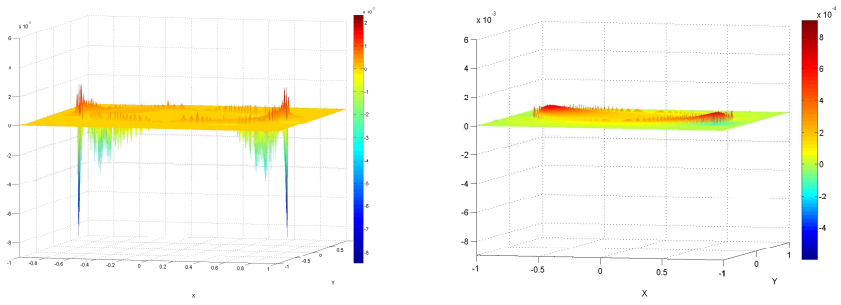

(a) P_1-IFEM (b) Modified P_1-IFEM

Figure 10: Error Surface for Example 6.3 (Variable coefficient) $(\beta^- = (x^2 + y^2 - 1)^2,\ \beta^+ = 1,\ 1/h_x = 128)$

3. Q_1-IFEM for rectangular elements.
4. 3-dimensional problems.
5. Problems with a moving interface.
6. Two phase Stokes/Navier-Stokes problems.
7. Development of fast solver such as multigrid methods.

Acknowledgments

This first author was supported by the National Research Foundation of Korea, No. 2014R1A2A1A11053889.

References

[1] D.N. Arnold, An interior penalty finite element method with discontinuous elements, *SIAM J. Numer. Anal.*, **19** (1982), 742-760.

[2] D.N. Arnold, F. Brezzi, B. Cockburn, D. Marini, *Discontinuous Galerkin methods for elliptic problems*, Springer, Berlin Heidelberg (2000).

[3] C.E. Baumann, J.T. Oden, A discontinuous hp finite element method for convection-diffusion problems, *Comput. Meth. Appl. Mech. Engrg.*, **175** (1999), 311-341.

	$1/h_x$	$\|u-u_h\|_0$	order	$\|u-u_h\|_{1,h}$	order	$\|u-u_h\|_\infty$	order
P_1-IFEM	8	8.550e-2		1.585e-0		2.415e-1	
	16	2.931e-2	1.544	9.840e-1	0.688	1.025e-1	1.237
	32	7.954e-3	1.882	5.538e-1	0.829	4.174e-2	1.295
	64	2.002e-3	1.990	3.033e-1	0.869	1.568e-2	1.413
	128	4.825e-4	2.053	1.665e-1	0.865	8.471e-3	0.888
	256	1.206e-4	2.000	8.948e-2	0.896	4.393e-3	0.947
	512	3.461e-5	1.802	5.063e-2	0.822	2.132e-3	1.043
	$1/h_x$	$\|u-u_h^m\|_0$	order	$\|u-u_h^m\|_{1,h}$	order	$\|u-u_h^m\|_\infty$	order
Modified P_1-IFEM	8	8.652e-2		1.572e-0		2.150e-1	
	16	2.867e-2	1.593	9.704e-1	0.696	9.448e-2	1.187
	32	8.049e-3	1.833	5.368e-1	0.854	3.656e-2	1.370
	64	2.195e-3	1.874	2.889e-1	0.894	1.097e-2	1.736
	128	5.585e-4	1.975	1.485e-1	0.959	3.055e-3	1.845
	256	1.437e-4	1.958	7.550e-2	0.976	8.386e-4	1.865
	512	3.649e-5	1.978	3.809e-2	0.987	2.209e-4	1.925

Table 5: Example 6.3 (Variable coefficient)

[4] D. Braess, *Finite elements: Theory, fast solvers, and applications in solid mechanics*, Second edition. Cambridge University Press, Cambridge (2001).

[5] J.H. Bramble, J.T. King, A finite element method for interface problems in domains with smooth boundary and interfaces, *Adv. Comp. Math.* **6** (1996), 109-138.

[6] S.C. Brenner, L.R. Scott, *The mathematical theory of finite element methods*, Springer-Verlag, New York (1994).

[7] K.S. Chang, D.Y. Kwak, Discontinuous Bubble scheme for elliptic problems with jumps in the solution, *Comput. Meth. Appl. Mech. Engrg.*, **200** (2011), 494-508.

[8] Z. Chen, J. Zou, Finite element methods and their convergence for elliptic and parabolic interface problems, *Numer. Math.* **79** (1998), 175-202.

[9] S.H. Chou, D.Y. Kwak, K.T. Wee, Some error estimates for an immersed interface finite element method, *unpublished manuscript (submitted to Comput. Meth. Appl. Mech. Engrg.)*, (2006).

[10] S.H. Chou, D.Y. Kwak, K.T. Wee, Optimal convergence analysis of an

immersed interface finite element method, *Adv. Comput. Math.*, **33** (2010), 149-168.

[11] P.G. Ciarlet, *The finite element method for elliptic problems*, North-Holland, Amsterdam, New York, Oxford (1978).

[12] M. Crouzeix, P.A. Raviart, Conforming and nonconforming finite element methods for solving the stationary Stokes equations, *RAIRO Anal. Numér.*, **7** (1973), 33-75.

[13] C. Dawson, S. Sun, M.F. Wheeler, Compatible algorithms for coupled flow and transport, *Comput. Meth. Appl. Mech. Eng.*, **194** (2004), 2565- 2580.

[14] J. Douglas, T. Dupont, Interior penalty procedures for elliptic and parabolic Galerkin methods, *Computing methods in applied sciences*, Springer, Berlin Heidelberg, (1976), 207-216.

[15] A. Hansbo, P. Hansbo, An unfitted finite element method, based on Nitsche's method, for elliptic interface problems, *Comput. Methods Appl. Mech. Engrg.*, **191** (2002), 5537-5552.

[16] S. Hou, X. Liu, A numerical method for solving variable coefficient elliptic equation with interfaces, *J. Comput. Phys.*, **202**, No. 2 (2005), 411-445.

[17] S. Hou, L. Wang, W. Wang, Numerical method for solving matrix coefficient elliptic equation with sharp-edged interfaces, *J. Comput. Phys.*, **229**, No. 19 (2010), 7162-7179.

[18] D.Y. Kwak, K.T. Wee, K.S. Chang, An analysis of a broken P_1 - nonconforming finite element method for interface problems, *SIAM J. Numer. Anal.*, **48** (2010), 2117-2134.

[19] M. Lai, Z. Li, X. Lin, Fast solvers for 3D Poisson equations involving interfaces in a finite or the infinite domain, *J. Comput. Appl. Math.*, **191**, No. 1 (2006), 106-125.

[20] Z. Li, T. Lin, X. Wu, New Cartesian grid methods for interface problems using the finite element formulation, *Numer. Math.*, **96** (2003), 61-98.

[21] Z. Li, T. Lin, Y. Lin, R.C. Rogers, An immersed finite element space and its approximation capability, *Numer. Methods. Partial Differential Equations*, **20** (2004), 338-367.

[22] Z. Li, K. Ito, *The immnersed interface method: Numerical solutions of PDEs involving interfaces and irregular domains*, Frontiers in Applied Mathematics, SIAM (2006).

[23] M. Oevermann, C. Scharfenberg, R. Klein, A sharp interface finite volume method for elliptic equations on Cartesian grids, *J. Comput. Phys.*, **228**, No. 14 (2009), 5184-5206.

[24] B. Riviére, M.F. Wheeler, V. Girault, Improved energy estimates for interior penalty, constrained and discontinuous Galerkin methods for elliptic problems I, *Comput. Geosci.*, **3** (1999), 337-360.

[25] J.A. Roitberg, Z.G. Seftel, A theorem on homeomorphisms for elliptic systems and its applications, *Math. USSR-Sb.* **7** (1969), 439-465.

[26] S. Yu, Y. Zhou, G.W. Wei, Matched interface and boundary (MIB) method for elliptic problems with sharp-edged interfaces, *J. Comp. Physics*, **224** (2007), 729-756.